ISBN: 978-3-95450-208-0 doi:10.18429/JACoW-IPAC2019-TUPMP013

NEW DESIGN OF VACUUM CHAMBERS FOR RADIATION SHIELD INSTALLATION AT BEAM INJECTION AREA OF J-PARC RCS

J. Kamiya†, H. Kotoku, Y. Shobuda, T. Takayanagi, K. Yamamoto, JAEA/J-PARC, Shirakata, Tokai, Naka, Ibaraki, Japan
T. Yanagibashi, K. Horino, N. Miki, NAT, Muramatsu, Tokai, Naka, Ibaraki, Japan

Abstract

One of the issues in the J-PARC 3 GeV rapid cycling synchrotron is the high residual radiation dose around the beam injection point. A radiation shield is necessary to reduce radiation exposure of workers when maintenance is performed there. A space to install the radiation shield should be secured by newly designing a structure of the vacuum chamber at the injection point and the alumina ceramics beam pipes for the shift bump magnets. To make the space for the shield, the chamber is lengthened along the beam line and the cross-sectional shape is changed from circle to rectangle. The displacement and inner stress of the vacuum chamber due to atmospheric pressure were evaluated to be enough small by the calculation. For the ceramics beam pipe's rf-shield, the damping resistor was effective to reduce the induced modulation voltages by the pulsed magnetic field.

INTRODUCTION

One of the issues in the J-PARC 3 GeV rapid cycling synchrotron (RCS) is the high residual radiation dose of the vacuum chambers and magnets in the beam injection area. The high radiation is caused by the nuclear scattering due to the interaction between the beam and a carbon foil for stripping the electrons of the injected H^- beam, which is called the 1st foil [1]. Fig. 1 shows a typical residual radiation distribution in the injection area. Residual dose in the downstream of the 1st foil is larger than that in the upstream due to the large scattering cross-section at the forward angle. The highest residual dose is estimated to be well over 15 mSv/h at the surface of the vacuum chamber at the beam injection point after the operation with an extracted beam power of 1 MW. The Effort to prevent workers radiation exposure during maintenance has been performed, such as a minimization of the foil hitting number [2], and control of the workers' radiation dosage by recording the pocket dosimeters value every entering and leaving the tunnel. However, against predicted higher residual dose for the future higher beam power operation, radiation shields around the 1st foil should be considered. The problem against consideration of the radiation shield is the limited space around the vacuum chamber at the injection point.

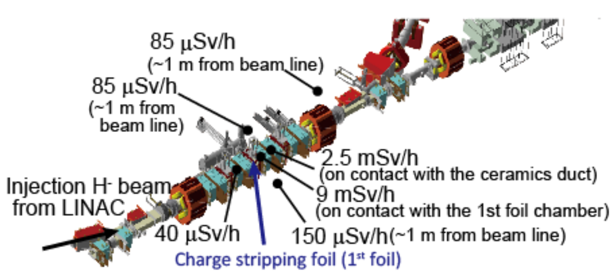

Figure 1: Typical residual dose distribution at the beam injection area in the RCS about 5 hours after beam operation with 500 kW power.

In this paper, the basic concept to make the space for the radiation shields and the related upgrade for the vacuum chamber and beam pipes are described. Firstly, the new configuration of the injection area under consideration is introduced. Next, the evaluation of the newly designed vacuum chamber at the injection point is described. Subsequently, the rf-shield on the alumina ceramics beam pipes, which is redesigned for the induced magnetic field damping, is mentioned.

NEW SYSTEM CONFIGURATION UNDER DESIGNING

Figure 2 a) shows the current configuration around the injection point. The 4 shift-bump magnets (SB1-4) create a bump orbit to match the injected H^- and circulating proton beam at the injection point. The beam orbit by the shift-bump magnets and the role of the 1st to 3rd charge stripping foil are described in the reference [3]. The 2nd foil strips the electron from the partially electron-stripped beam by the 1st foil, H^0. The current SB4 core is a split type to insert the 2nd foil in the middle of the SB4. SB1-3 are designed to be the same as SB4 for mass production. Orbit calculation showed that the partially electron-stripped beam, H^0, cannot be transported to the injection beam dump if the position of the 2nd foil is changed to upstream or downstream of the SB4. Therefore, as shown in Fig. 2 b), even in the new design, the SB4 core should be a split type. Only the SB2 and SB3 cores are changed to the combined

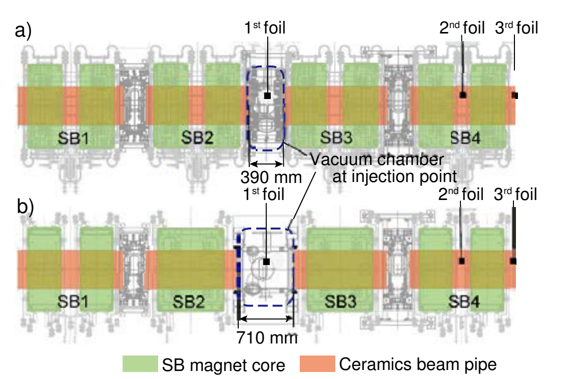

Figure 2: System configuration of the beam injection area. a) Current configuration. b) New configuration under designing for the radiation shield installation.

† email address: junichiro.kamiya@j-parc.jp

ISBN: 978-3-95450-208-0 doi:10.18429/JACoW-IPAC2019-TUPMP013

type to make space around the injection point, while the SB1 and SB4 cores remain split type. As a result, the chamber can be lengthened from 390 mm to 710 mm to the beam direction to secure the shield space.

VACUUM CHAMBER AT BEAM INJECTION POINT

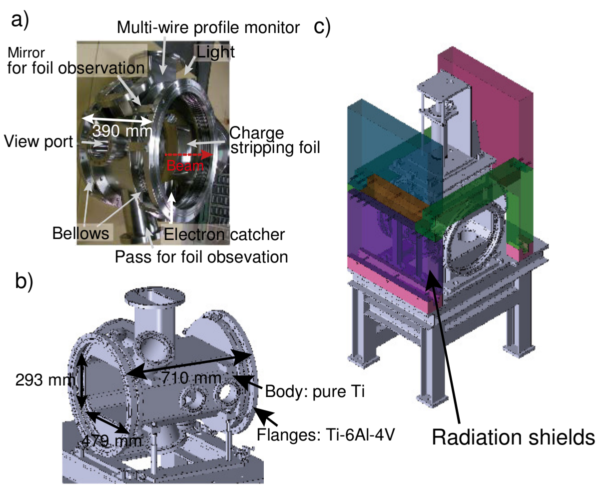

Figure 3: a) Current vacuum chamber at the beam injection point. b) Newly designed vacuum chamber. c) Radiation shield under designing.

Figure 3 a) and b) show the current and newly designed vacuum chamber at the beam injection point, respectively. Radiation shields under designing are also shown in Fig. 3 c). The cross-sectional shape was changed from circle to rectangle with a vertical and horizontal sides of 293 mm and 479 mm in outline, respectively, to make shield space. Pure titanium of Japan Industrial Standard (JIS) Class 2 (Ti Class 2) is used for the body, ports, bellows because the titanium is low radioactivation material. Titanium alloy of JIS Class 60 (Ti-6Al-4V) is used for the flanges due to its high mechanical strength and hardness to avoid to dent by the metal vacuum seal. Vickers hardness of Ti-6Al-4V is about 320 HV, while that of Ti Class 2 is about 160 HV. It is necessary to check the displacement and inner stress for

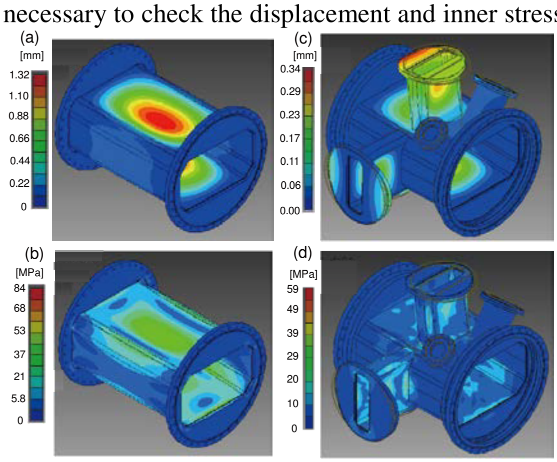

Figure 4: a), b) Calculated displacement and Von Mises stress in a vacuum chamber without bellows and ports. c), d) Those in the vacuum chamber with the final design.

the chamber by the atmospheric pressure because the chamber was designed to be longer and its cross-sectional shape to be a rectangle. First, the thickness of the chamber's rectangular body was decided to be enough thick for the displacement by the atmospheric pressure not to be larger than 1.5 mm. The Finite Element Method (FEM) analysis was performed for the simple shape without ports. Fig. 4 a) and b) shows the calculated displacement and inner stress in the case of 9 mm thickness. With this thickness, the maximum displacement is within about 1.3 mm and the maximum inner stress is about 95 MPa, which is enough smaller than the yield point of Ti Class 2, >216 MPa. To check the validity of the calculation, the vacuum chamber with the same shape as the calculation was produced and the displacement was measured when it was evacuated. Fig. 5 shows the comparison of the calculated displacement of the chamber by the atmospheric pressure with the measured one. The calculation is well reliable because it agrees well with the measurement. Followed by this result, the deformation and stress were calculated for the actual shape of the vacuum chamber, which has a number of ports on the body. As shown in Fig. 4 b) and c), it was confirmed that there is no problem for both displacement and inner stress in the vacuum chamber with the final design.

The other verification point is the heat generation by the leakage pulsed magnetic field of the SB. Because the vacuum chamber wall comes closer to the medium plane due to the shape change from the circle to rectangle, the vertical component of the leakage magnetic field which path through the vacuum chamber wall increases comparing to the present status. The calculation showed that the heat generation in the vacuum chamber body increases from 12 W to 74 W. The temperature increase by the 74 W heat generation is estimated to be about 60°C, fortunately, which will not be going to matter.

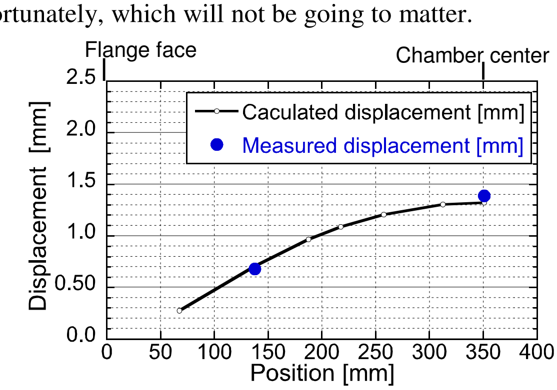

Figure 5: Calculated and measured displacement by the atmospheric pressure of the vacuum chamber.

RF-SHIELD ON CERAMICS BEAM PIPES

The ceramics beam pipes are used for the SB. The rf-shield, which consists of copper stripes with capacitors, is equipped on the outer surface of the ceramics beam pipes. The stripes have a role of propagating the mirror current of the beam to reduce the impedance affecting on the beam, while the capacitors cut the induced current by the time-

ISBN: 978-3-95450-208-0 doi:10.18429/JACoW-IPAC2019-TUPMP013

variable magnetic field in the stripes at a lower frequency. The time constant τ of the induced current modulation for the equivalent electrical circuit of the rf-shield is $2L/R$, where the L and R are the inductance and resistor of the stripe. Due to the large τ, a few ms, the modulation of the magnetic field by the induced current exist in time region where the beam exists. In the current system shown in Fig. 2 a), the modulation of the induced magnetic field is canceled between SB1 and 2 (SB3 and 4), due to the symmetric structure. However, in the new design in Fig. 2 b), the modulation cannot be canceled due to the asymmetricity of SB1 and 2 (SB3 and 4) magnetic field distribution. It would generate an unwanted bending angle to the beam orbit and lead to serious beam loss. To overcome this problem, the active damping scheme was proposed [4]. In the scheme, damping resistors are installed in parallel with each capacitor. The time constant τ of the circuit is expressed as

$$\tau = \frac{2}{\left(\frac{R}{L} + \frac{1}{R'C}\right)} \sim 2CR',$$

where the C and R' are the capacitance of the capacitor and ohmic value of the additional resistor for modulation damping, respectively. Thus, the faster damping speed is obtained with smaller resistor value. However, on the other hand, the power consumption P in the resistor increases with the smaller resistor value according to $P = V^2/R'$, where V is the induced voltage. Therefore, the combination way of the resistors should be decided to obtain enough fast damping speed within the allowable power consumption in the resistor.

To examine the combination way of the resistor, the voltage on the resistor and the resistor temperature were measured using an rf-shield mock-up. In the measurement, the rf-shield mock-up was installed in the newly designed SB2, 3 type magnet and the R&D power supply. The actual excitation current pattern is 400 µs in rise time, 800 µs in flat top, and 370 µs in fall time, respectively, with the flat top current of 16 kA. In the experiment, due to the specification limit of R&D power supply, the pattern was fixed to 800, 100, 800 µs for rise time, flat top, fall time, respectively, with the maximum flat top current of 9.5 kA. Fig. 6 shows the measured modulation of the induced voltage dependence on the resistor value. The damping speed dependence on the resistor value was clearly

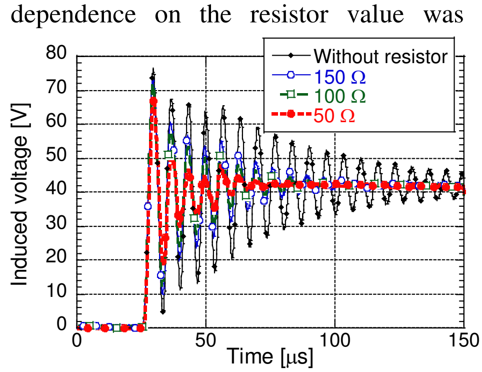

Figure 6: Dependence of the induced voltage modulation on the damping resistor value. The flat top excitation current was 9.5 kA .

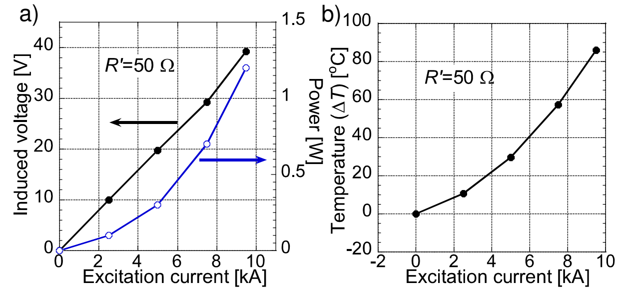

Figure 7: a) Dependence of the voltage and power of a dumping resistor on the excitation current. b) Dependence of the damping resistor temperature on the excitation current.

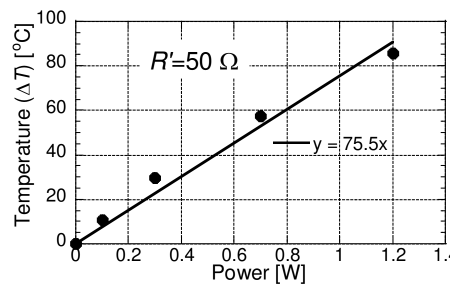

Figure 8: Relation of the temperature rise and power consumption of the 50 Ω resistor. The dots are measured value and the line is the linear fit.

observed. Based on this result, it is now under estimation how small resistor value is necessary to suppress the unwanted bending angle to the beam. Here we discuss the combination way of the resistor on the assumption that the total resistor value should be 50 Ω. Fig. 7 a) shows the voltage and power dependence on the excitation current, while Fig. 7 b) is the temperature dependence on the excitation current. Fig. 8 represents the relation of temperature and power consumption. The rating temperature rise and power consumption of a selected resistor are about 90°C and 3 W, respectively. From Fig. 8, the temperature limits the maximum allowable power consumption within about 1.2 W. The power consumption in the case of the actual excitation current pattern is estimated to be 6.7 W. Therefore, one solution for the resistor combination way to obtain the total damping resistor value of 50 Ω is 7 series of 7.1 Ω resistor, which produces less than 1 W power consumption per resistor.

CONCLUSION

The vacuum chamber at the beam injection point was newly designed to secure enough space for the radiation shields. The calculation showed that the deformation, inner stress, and temperature rise of the vacuum chamber are enough within the allowable ranges. The rf-shield on the ceramics beam pipe was considered with the active damping resistor. The measured temperature and power of the resistor gave the information for deciding the combination way of enough small resistors not to generate the unwanted bending angle to the beam orbit.

ISBN: 978-3-95450-208-0 doi:10.18429/JACoW-IPAC2019-TUPMP013

REFERENCES

[1] I.Sugai *et al.*, "Double-layer effects on the lifetime of newly developed HBC-foils for RCS of J-PARC", *Nucl. Instr. Meth. A*, vol. 613, pp. 457-461, 2010.

[2] H.Hotchi *et al*., "Achievement of a low-loss 1-MW beam operation in the 3-GeV rapid cycling synchrotron of the Japan Proton Accelerator Research Complex", *Phys. Rev. Accel. Beams*, vol. 20, p. 060402, 2017.

[3] P. K. Saha *et al*., "State of the art online monitoring system for the waste beam in the rapid cycling synchrotron of the Japan Proton Accelerator Research Complex", *Phys. Rev. Accel. Beams*, vol. 14, p. 072801, 2011.

[4] Y. Shobuda and Y. Irie, "Analytical estimation of the field modulation during the injection period of the 3 GeV RCS in J-PARC", in *Proc. 2nd Int. Symp. Science at J-PARC,* Tsukuba, Japan, Jul. 2014, p. 012003.